

Space Vector PWM and Model Predictive Control for Voltage Source Inverter Control

Irtaza M. Syed, Kaamran Raahemifar

Abstract—In this paper, we present a comparative assessment of Space Vector Pulse Width Modulation (SVPWM) and Model Predictive Control (MPC) for two-level three phase (2L-3P) Voltage Source Inverter (VSI). VSI with associated system is subjected to both control techniques and the results are compared. Matlab/Simulink was used to model, simulate and validate the control schemes. Findings of this study show that MPC is superior to SVPWM in terms of total harmonic distortion (THD) and implementation.

Keywords—Model Predictive Control, Space Vector Pulse Width Modulation, Voltage Source Inverter.

I. INTRODUCTION

THE DC to AC power converters are known as inverters. Inverters are mainly classified as current and voltage source inverters. Current source inverters have DC current source at input and use switches to adjust the output current and frequency. On the hand, voltage source inverters (VSI) convert DC power into AC power at desired voltage and frequency [1]. The AC output voltage and frequency may be fixed or variable depending on the application [2]. Semiconductor switches, such as Bipolar Junction Transistors, Metal Oxide Semi-conductor Field Effect Transistors, Insulated Gate Bipolar Transistors, etc., are used to control and adjust the output parameters [3]. Anti-parallel diodes are connected across from the switches to add a reverse current capability [2]. VSI requires a stiff DC voltage source at input [1] for quality operation. The input source could be the output of a rectifier, battery, fuel cell, or photo voltaic (PV) system.

Fig. 1 shows a basic two-level three phase (2L-3P) VSI circuit, where P is positive, N is negative terminal and O is a null point. VSI has three legs each with two switches and two anti-parallel diodes. For example, leg-1 has switches 1 (S₁) and 4 (S₄) and diodes 1 (D₁) and 4 (D₄). To prevent short circuit across terminals switches of the same leg should never be turned on simultaneously. Therefore, intentional switching delay (known as dead or blanking time) is introduced to ensure the first switch is turned off before the complementary switch of the same leg is turned on. If a short circuit happens, the fault current rises very quickly and unless it is controlled by proper protecting measures, it can damage the system. Similarly, switches of the same leg are never turned off

simultaneously to avoid uncertain output voltage. Terminals A, B, C can be connected to three phase load or across grid depending on off-grid or on-grid operation.

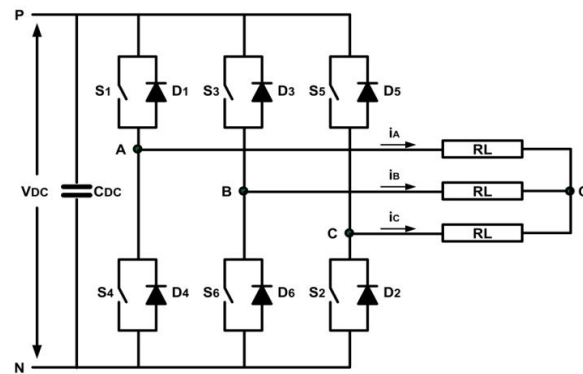


Fig. 1 2L-3P VSI basic circuit

Though the output voltage can be controlled by adjusting V_{DC} , usually the more convenient method of Pulse Width Modulation (PWM) is used. PWM adjusts pulse width by increasing or decreasing on and off times of the switches to control the output voltage. Conventionally, the on and off commands are issued by comparing three phase modulating signals (V_{mA} , V_{mB} , V_{mC}) with a carrier wave (V_c) (1).

$$V_{xN} = \begin{cases} V_{DC} & \text{if } V_{mx} > V_c \\ 0 & \text{if } V_{mx} < V_c \end{cases} \quad (1)$$

where $x=A,B,C$

For example, if $V_{mA} > V_c$, $V_{AN} = V_{DC}$ with S_1 on and S_4 off. On the other hand, if $V_{mA} < V_c$, $V_{AN} = 0$ with S_1 off and S_4 on. The status of switches for all three legs is shown in Table I.

TABLE I
THE STATUS OF SWITCHES IN INDIVIDUAL LEGS

THE STATES OF SWITCHES IN INDIVIDUAL LEGS									
S States	Leg A			Leg B			Leg C		
	S ₁	S ₄	V _{AN}	S ₃	S ₆	V _{BN}	S ₅	S ₂	V _{CN}
P	1	0	V _{DC}	1	0	V _{DC}	1	0	V _{DC}
O	0	1	0	0	1	0	0	1	0

Since the input lines should never be shortened and the output current should always be continuous, a voltage source inverter can assume only 8 distinct switching states, defined by (2) and presented in Table II.

$$\text{States} = n^3 \quad (2)$$

where $n=2$ for two level VSI.

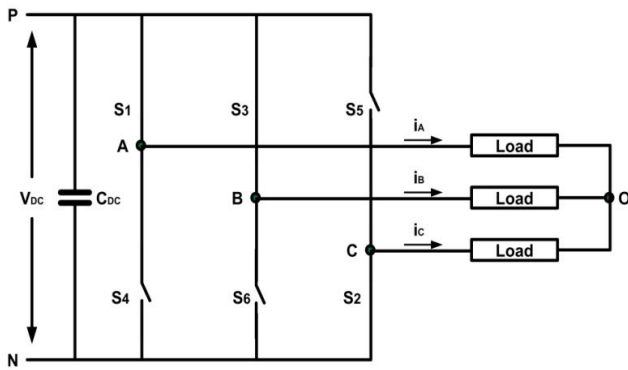
Irtaza M. Syed is a student at the Electrical & Computer Engineering Department, Ryerson University, Toronto, ON M5K 2K3 Canada (corresponding author phone: 647-787-6262; e-mail: isyed@ryerson.ca).

Dr. Kaamran Raahemifar, is with the Electrical & Computer Engineering Department, Ryerson University, Toronto, ON M5K 2K3 Canada, (e-mail: kraahemi@ee.ryerson.ca).

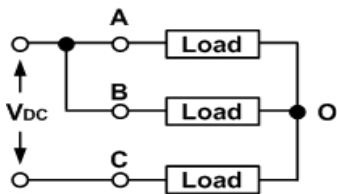
TABLE II
VSI 8 SWITCHING STATES

Legs Upper S			Legs Lower S			Voltage		
S ₁	S ₃	S ₅	S ₄	S ₆	S ₂	V _{AN}	V _{BN}	V _{CN}
0	0	0	1	1	1	V _{DC}	V _{DC}	V _{DC}
0	0	1	1	1	0	V _{DC}	V _{DC}	0
0	1	0	1	0	1	V _{DC}	0	V _{DC}
0	1	1	1	0	0	V _{DC}	0	0
1	0	0	0	1	1	0	V _{DC}	V _{DC}
1	0	1	0	1	0	0	V _{DC}	0
1	1	0	0	0	1	0	0	V _{DC}
1	1	1	0	0	0	0	0	0

Individual phase voltages on the load can easily be determined considering the fact that any switching combination will result in a specific configuration of the VSI circuit. Fig. 2 shows VSI circuit configuration when $S_1S_2S_3=111$.

Fig. 2 VSI circuit for $S_1S_2S_3=111$

Alternatively, the VSI circuit configuration when $S_1S_2S_3=111$ can be shown as in Fig. 3. Phase A and B are connected to the positive terminal of V_{DC} while phase C is connected to the negative terminal of V_{DC} and all three of them are connected to O (null) point through load. This configuration puts load A and B in parallel, connected in series with load C and the DC source. Thus load phase voltages $V_{AO}=V_{BO}=1/3V_{DC}$ and $V_{CO}=-2/3V_{DC}$. Fig. 4 shows the equivalent circuit for $S_1S_6S_2=111$, producing $V_{AO}=2/3V_{DC}$ and $V_{BO}=V_{CO}=-1/3V_{DC}$. It is important to note that $V_{AO}=V_{BO}=V_{CO}=0$ for both $S_1S_3S_5=111$ ($S_4S_6S_2=000$) and $S_1S_3S_5=000$ ($S_4S_6S_2=111$).

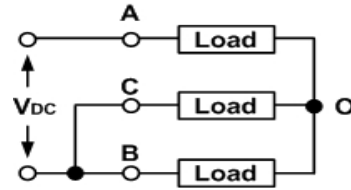
Fig. 3 VSI circuit for $S_1S_2S_3=111$

Line to line voltages (V_{AB} , V_{BC} , V_{CA}) are obtained by subtracting line to neutral voltage of one phase from the other. For example, V_{AB} is calculated by (3). Table III shows the

phase load voltages and line to line voltages.

$$V_{AB} = V_{AN} - V_{BN} \quad (3)$$

Multiple methods exist for controlling VSI. This paper compares Space Vector Pulse Width Modulation (SVPWM) with Model Predictive Control (MPC) for VSI. The rest of the paper is organized into the following sections: (II) DQ transformation, (III) SVPWM, (IV) MPC, (V) System Performance Assessment, (VI) Results and Discussion, (VII) Conclusions.

Fig. 4 VSI circuit for $S_1S_6S_2=111$

II. DQ TRANSFORMATION

In a balanced three phase system, the sum of three phase voltage (or current) equals to zero due to the equal amplitude and 120° phase shift (4). This renders one of the three V_s (or I_s) redundant. Therefore, if the value of two voltages (or currents) is known, the third one can be found. This redundancy permits conversion of the three phase (or three frames) ABC variables to two frames $\alpha\beta$ (or $\alpha\beta 0$) and dq (or $dq 0$) variables.

$$X_{AO} + X_{BO} + X_{CO} = 0 \quad (4)$$

TABLE III
PHASE LOAD AND LINE TO LINE VOLTAGES

Lower leg Sw			Phase load V*			Line-Line V*		
S ₄	S ₆	S ₂	V _{AO}	V _{BO}	V _{CO}	V _{AB}	V _{BC}	V _{CA}
1	1	1	0	0	0	0	0	0
1	1	0	-1/3	-1/3	2/3	0	-1	1
1	0	1	-1/3	2/3	-1/3	-1	1	0
1	0	0	-2/3	1/3	1/3	-1	0	1
0	1	1	2/3	-1/3	-1/3	1	0	-1
0	1	0	1/3	-2/3	1/3	1	-1	0
0	0	1	1/3	1/3	-2/3	0	1	-1
0	0	0	0	0	0	0	0	0

* multiply all V's V_{DC}

Converting the three phase control problem into two phase control problem makes analysis, design and control of the VSI and the associated system simple. Although $\alpha\beta$ conversion reduces one phase and therefore simplifies the system control, the two dimensional frame remains sinusoidal. On the other hand dq synchronous not only results in two phase but a DC control problem, enabling use of PID controllers. dq transformation in any reference frame can be obtained by (5) and (6). Theta (θ) is used to define the reference frame: the reference frame is Stationary ($\alpha\beta$) if $\theta=0$, Synchronous if $\theta=\theta_{grid}$ and Arbitrary if θ is neither zero nor equal to θ_{grid} . The $\alpha\beta$ reference frame is used to control VSI in both SVPWM and

MPC.

Equation (5) gives the transformation from ABC to dq (direct), while (6) gives the transformation from dq to ABC (inverse).

$$\begin{bmatrix} X_d \\ X_q \end{bmatrix} = \frac{2}{3} \begin{bmatrix} \cos\theta & \cos(\theta - \frac{2\pi}{3}) & \cos(\theta - \frac{4\pi}{3}) \\ -\sin\theta & -\sin(\theta - \frac{2\pi}{3}) & -\sin(\theta - \frac{4\pi}{3}) \end{bmatrix} \begin{bmatrix} X_a \\ X_b \\ X_c \end{bmatrix} \quad (5)$$

$$\begin{bmatrix} X_a \\ X_b \\ X_c \end{bmatrix} = \begin{bmatrix} \cos\theta & -\sin\theta \\ \cos(\theta - \frac{2\pi}{3}) & -\sin(\theta - \frac{2\pi}{3}) \\ \cos(\theta - \frac{4\pi}{3}) & -\sin(\theta - \frac{4\pi}{3}) \end{bmatrix} \begin{bmatrix} X_d \\ X_q \end{bmatrix} \quad (6)$$

where $X=V, I$, etc.

III. SVPWM

Sinusoidal PWM (SPWM), a very popular technique, creates a relatively high harmonic distortion due to its asymmetrical nature of the PWM switching and cannot make use of the inverter's supply voltage fully [3]. SVPWM however, provides a higher voltage and lower total harmonic distortion (THD) and is therefore, preferred.

SVPWM control strategy is based on the fact that the VSI possible switching states are finite. The 2L-3P VSI has 6 active and 2 zero space (or voltage) vectors. The six active vectors produce a nonzero output voltage and the two zero vectors produce zero output voltage (Table IV).

TABLE IV
VSI SPACE VECTORS

S_4	S_6	S_2	Vector	V_x
1	1	1	0	V_0
1	1	0	$2/3V_{DC}$	V_1
1	0	1	$1/3V_{DC} + j\sqrt{3}/3V_{DC}$	V_2
1	0	0	$-1/3V_{DC} + j\sqrt{3}/3V_{DC}$	V_3
0	1	1	$-2/3V_{DC}$	V_4
0	1	0	$-1/3V_{DC} - j\sqrt{3}/3V_{DC}$	V_5
0	0	1	$1/3V_{DC} - j\sqrt{3}/3V_{DC}$	V_6
0	0	0	0	V_7

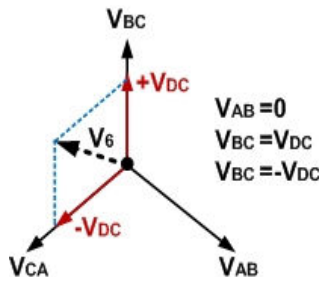


Fig. 5 Space vector V_6

Space vector of the three phase quantities are represented as vectors in a two-dimensional $\alpha\beta$ plane. For example, V_6 shown in Fig. 5 represents $S_1S_2S_3=111$ (Figs. 2 & 3) or vector V_6 ($S_4S_6S_2=001$) in Table III. V_{AB} , V_{BC} , and V_{CA} are three 120° phase shifted line voltage vectors, represented by $V_{AB}=0$, $V_{BC}=V_{DC}$ and $V_{CA}=-V_{DC}$ for this case (Fig. 5) with an effective voltage(space) vector V_6 equal to $1/3V_{DC} - j\sqrt{3}/3V_{DC}$. In general,

$$\vec{X} = X_\alpha + jX_\beta \quad (7)$$

Proceeding on similar lines the six non-zero voltage vectors ($V_1 - V_6$) can assume the positions shown in Fig. 6, forming a regular hexagon. There are six active vectors, with the area between any two adjacent vectors defined as a sector. The remaining two zero space vectors produce no output voltage, and therefore they remain at origin in $\alpha\beta$ plane defining no sector. Space vector V is known as the reference space vector.

Note that all the 8 space vectors are stationary. The reference space vector, V (equivalent of V_α and V_β at angle α), however rotates in space at angular velocity of ω (or $2\pi f$). At any time, V is approximated by two active space vectors and a zero space vector. V rotates one revolution for one complete cycle of V_{AB} and its length corresponds to the magnitude of V_{AB} .

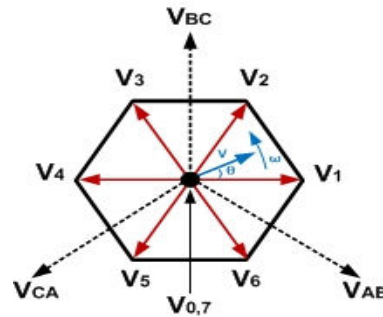


Fig. 6 SVPWM space vectors

To generate any magnitude of V_{AB} at the specific angle α , V_α and V_β followed by V and α are determined using (5), (8) and (9). Then the turn on durations T_1 , T_2 , and T_0 are estimated with appropriate switching sequence and switching time for switches (S_1-S_6) using (10) to (12).

$$\vec{V} = \sqrt{V_\alpha^2 + V_\beta^2} \quad (8)$$

$$\alpha = \tan^{-1} \frac{V_\beta}{V_\alpha} = \omega t = 2\pi f t \quad (9)$$

$$T_1 = \frac{\sqrt{3}T|V|}{V_{DC}} \left(\sin \frac{n\pi}{3} \cos \alpha - \cos \frac{n\pi}{3} \sin \alpha \right) \quad (10)$$

$$T_2 = \frac{\sqrt{3}T|V|}{V_{DC}} \left(-\cos \alpha \sin \frac{(n-1)\pi}{3} + \sin \alpha \cos \frac{(n-1)\pi}{3} \right) \quad (11)$$

$$T_0 = T - T_1 - T_2 \quad (12)$$

where $T = 1/f$, $n=1-6$ (sectors), and $0 \leq \alpha \leq 60^\circ$ [4].

There are a few options for null vector: V_0 only, V_7 only, or a combination of both [5]. The type of null vector determines the SVM technique. Based on the type of null vector different SVPWM techniques such as right aligned, symmetric, alternating zero vector and highest current not switched sequences [5] are obtained. All the techniques have almost identical DC source utilization; however, they differ in terms of switching loss and THD. Usually the optimal choice is 7-segment switching sequence (Fig. 7) which ensures minimum switching per sampling period and low harmonics.

IV. MPC

Model predictive control strategies like SVPWM take advantage of the fact that only a finite number of possible switching states are associated with VSI. These states are discrete and the model of the system can be used in association with a discrete-time model of the load to predict the behavior of the VSI system. A selection criterion, the objective function, is defined for selection of the optimal future variables corresponding to the optimal future switching state that minimizes the objective function. The objective of the MPC scheme is to predict switching state and thus currents that track the reference currents with minimal error. For each sampling period predicted, the output currents are measured and compared with the reference currents to minimize error. Usually the sampling period is chosen as a period in which the reference current does not change significantly; therefore, the reference current can be considered a constant for that period.

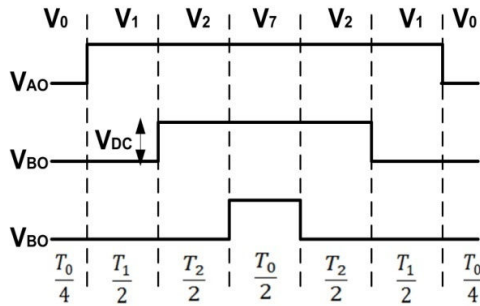


Fig. 7 SVPWM with seven segment switching sequence

All the VSI operational requirements and constraints outlined in Sections I and II are still valid except for the control scheme. Similar to SVPWM, MPC is exercised in $\alpha\beta$ reference frame with 6 active and 2 zero vectors. In addition, load dynamics are modeled as:

$$v = L \frac{di}{dt} + Ri \quad (13)$$

where R and L are load resistance and inductance, respectively, i is the load current and v is the VSI generated voltage vector.

Using Euler-Forward equation, the load current is approximated by:

$$\frac{di}{dt} \cong \frac{i(k+1) - i(k)}{T} \quad (14)$$

From (13) and (14), we can say:

$$i^p(k+1) = \left(1 - \frac{RT}{L}\right)i(k) + \frac{T}{L}v(k) \quad (15)$$

where $k=t$ (present) and $k+1=t+1$ (future/predicted). Using (5), the predicted load current in (15) can be expressed in the $\alpha\beta$ reference frame as:

$$\begin{bmatrix} i_{\alpha(k+1)} \\ i_{\beta(k+1)} \end{bmatrix} = \begin{bmatrix} 1 - \frac{RT}{L} & 0 \\ 0 & 1 - \frac{RT}{L} \end{bmatrix} \begin{bmatrix} i_{\alpha(k)} \\ i_{\beta(k)} \end{bmatrix} + \begin{bmatrix} \frac{T}{L} & 0 \\ 0 & \frac{T}{L} \end{bmatrix} \begin{bmatrix} v_{\alpha(k)} \\ v_{\beta(k)} \end{bmatrix} \quad (16)$$

Equation (16) is used to predict the load current for each switching possibility. The objective function is evaluated for each of the eight possible voltage vectors generated by the VSI in order to calculate the future optimal value of the load current. The optimal value of the objective function is applied during the next sampling period. Fig. 8 shows the VSI MPC control system.

Fig. 9 outlines step by step implementation process of MPC for predictive control of VSI. First all the variables are initialized and values assigned (Data). This is followed by a process dynamic model of VSI based on the values for voltage vectors V_0 to V_7 (Table IV). Then a set of control actions or manipulated variables $U_{(k)}$ based on operational principles (process experience) is developed corresponding to all possible output states (using switching states, $S_4S_6S_2$) in Table IV. Current states of the system are measured (i_{0-ref} , $i_{0(k)}$) including switching states of $v_{(k)}$ and future outputs $Y_{(k+1)}$ (future currents $i_{0(k+1)}$) for $k=1$ to N are predicted using (16).

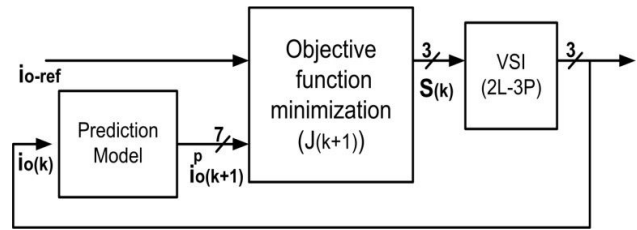


Fig. 8 VSI MPC control block diagram

Objective function J (17) is used to minimize the error between predicted output, $Y_{(k)}$ and the measured reference, i_{0-ref} ($r_{(k)}$). The optimal $J_{(k+1)}$ with minimum error between predicted and measured currents is selected and the corresponding control action, $U_{(k)}$, from the control action set, $U = [000\ 001\ 010\ 011\ 100\ 101\ 110\ 111]$, is applied across VSI in the next sampling period. The output is observed and the process is repeated. Note that in each sampling period 8 predictions are made and 8 Js are evaluated before selecting the control action, $U_{(k)}$, for the next sampling period.

$$\min J_{(k+1)} = \sum_{k=1}^{k+N-1} (Y_{(k)} - r_{(k)}) \quad (17)$$

V. SYSTEMS PERFORMANCE ASSESSMENT

VSI output is ideally sinusoidal and independent of load parameters; however, the output of the practical inverter is non-sinusoidal and contains harmonics. The performance of VSI is therefore evaluated in terms of total harmonic distortion (THD), Distortion Factor (DF), and lower harmonic distortion (LOH) [3]. In addition, power loss, control complexity, implementation ease, and cost are also considered when evaluating VSI and the associated control plan.

The ratio of the root mean square (rms) and sum of total harmonic components of output voltage plus rms of the fundamental component, V_{of} , is called THD. It is the measure of closeness in shape between a waveform and its V_{of} . The LOH is the harmonic component with a magnitude greater than or equal to 3% of V_{of} .

$$THD = \frac{1}{V_{of}} (\sum_{n=2,3...}^{\infty} V_{on}^2)^{1/2} \quad (18)$$

To compare SVPWM and MPC control for 2L-3P VSI, Advanced Energy AE 100TX, a commercially available VSI from [6] with rated kVA= 100kW, rated $V_{LL} = 600V$, rated $I_o = 96A$, and $f=60$ Hz is selected.

For $m_a=1.0$, DC link voltage is:

$$V_{DC} = \sqrt{2} \frac{V_{LL}}{m_a} \cong 850 V \quad (19)$$

Using per unit system, the base quantities are:

$$V_B = \frac{V_{LL}}{\sqrt{3}} = 347 V \quad (20)$$

$$I_B = \frac{S_R}{\sqrt{3}V_{LL}} = 96 A \quad (21)$$

$$Z_B = \frac{V_B}{I_B} = 3.62 \Omega \quad (22)$$

$$\omega_B = 2\pi f = 376.8 \text{ rad/s} \quad (23)$$

$$L_B = \frac{Z_B}{\omega_B} = 9.6 \text{ mH} \quad (24)$$

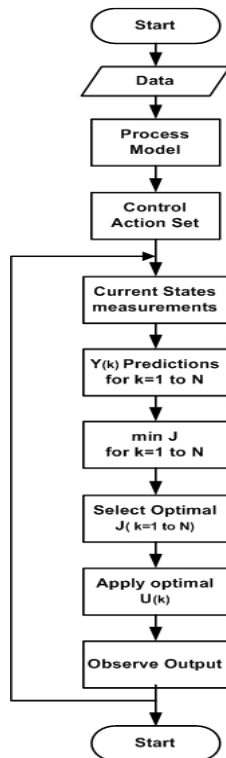


Fig. 9 MPC algorithm

For 1 pu load impedance, L_L is 0.31 pu and R_L equals to 0.95 pu, given by (25) and (26):

$$L_L = 0.31L_B \cong 3 \text{ mH} \quad (25)$$

$$R_L = 0.31Z_B \cong 3.44 \Omega \quad (26)$$

Finally sampling time, T_s , is set to $5\mu s$ for simulation. Fig. 10 shows the system modelled and simulated for both SVPWM and MPC.

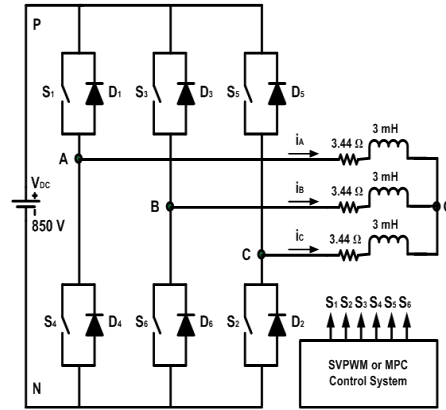


Fig. 10 VSI system simulated

VI. SIMULATION RESULTS

Fig. 11 (top panel) shows the output of VSI with SVPWM control and without LC filter (NF). Phase a current, I_a , is not a pure sine wave and contains harmonics. The middle and bottom panels of Fig. 11 show V_{ab} and V_a , respectively.

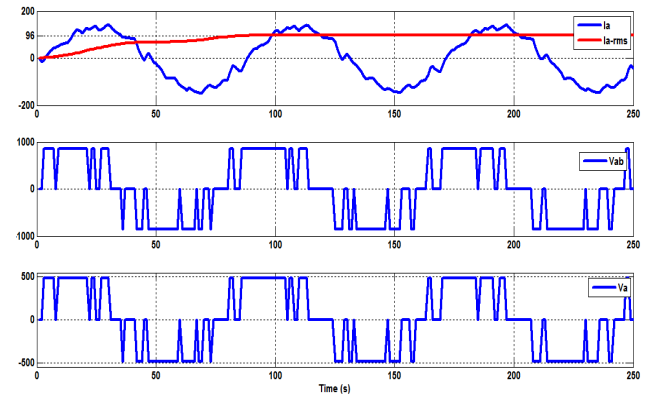


Fig. 11 I_a , I_a -rms, V_{ab} , and V_a (SVPWM-NF)

Fig. 12 shows I_a THD analysis. I_a is not a pure sine wave and contains harmonics. Fundamental component (f_c) has a peak magnitude of 135.4 with 10.98% THD.

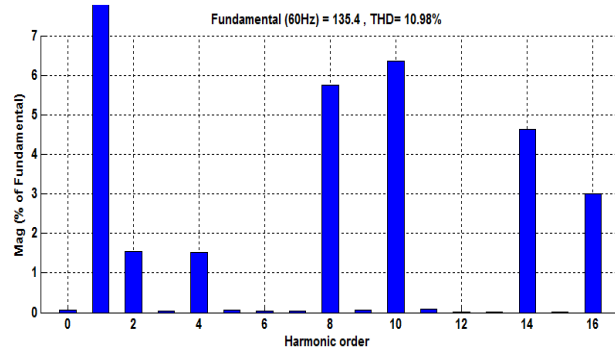


Fig. 12 Fundamental and THD of I_a (SVPWM-NF)

Fig. 13 presents the results of the same analysis for V_a and shows that V_a has f_c of 490.2 with a THD equal to 51.68%.

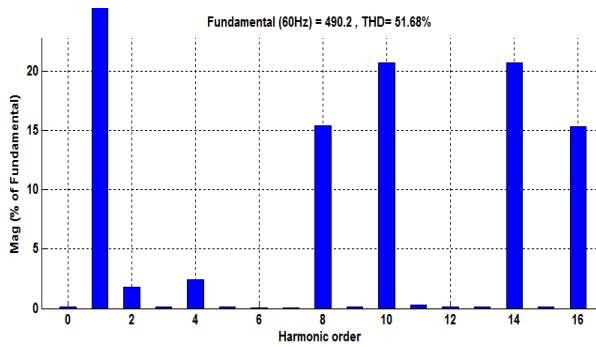
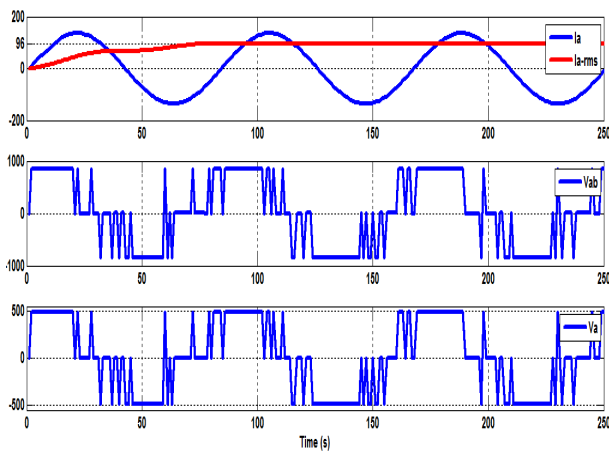
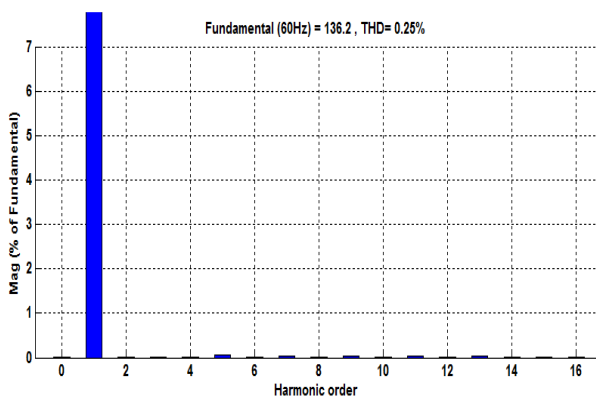
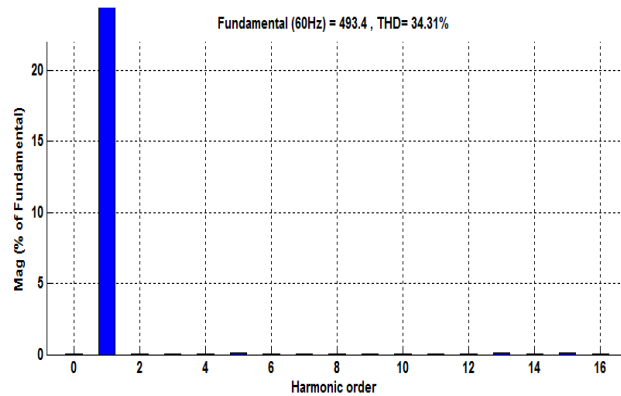
Fig. 13 Fundamental and THD of V_a (SVPWM-NF)

Fig. 14 shows the output of VSI with MPC control and without LC filter (NF). Note that I_a is almost a pure sine wave, even without an LC filter.

Fig. 14 I_a , I_{a-rms} , V_{ab} , and V_a (MPC-NF)

Figs. 15 and 16 show I_a and V_a fc and THD analysis. Both figures indicate great improvement in THD which is down from 10.98% to 0.25% and 51.68% to 34.31% for I_a and V_a respectively.

Fig. 15 Fundamental and THD of I_a (MPC-NF)Fig. 16 Fundamental and THD of V_a (MPC-NF)

Figs. 17 and 18 show VSI output with SVPWM and MPC controls with LC filter (YF). The inductor (L) and capacitor (C) used are 4 mH and 370 μ F respectively. Closer observation of Fig. 17 reveals that as expected $I_{a-rms}=96$ A, $V_{ab-rms}=600$ V and $V_{a-rms}=347$ V; however, there is slight harmonics mix. Fig. 18 shows the same results for I_{a-rms} , V_{ab-rms} and V_{a-rms} with less harmonics.

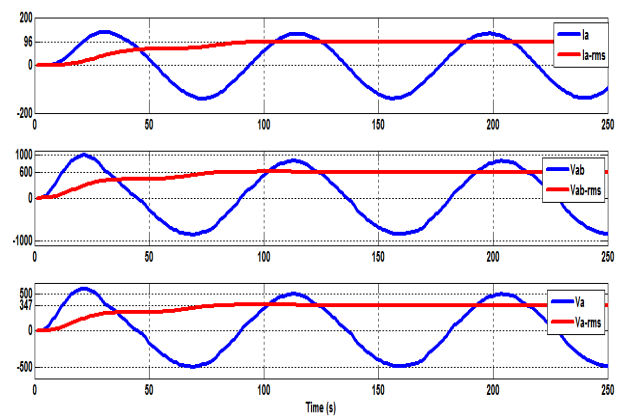
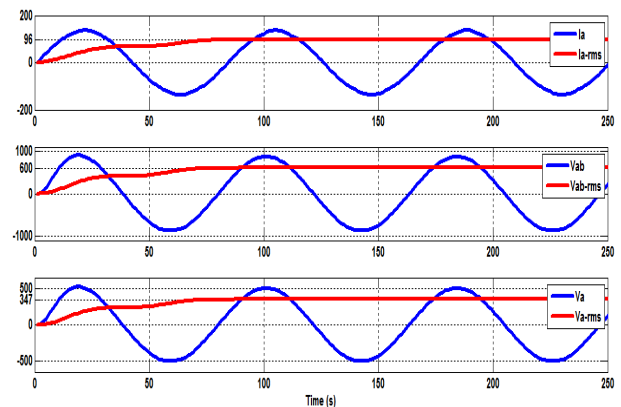
Fig. 17 I_a , I_{a-rms} , V_{ab} , and V_a (SVPWM-YF)Fig. 18 I_a , I_{a-rms} , V_{ab} , and V_a (MPC-YF)

Table V lists fc magnitude and THD for the waveforms in Figs. 17 and 18.

TABLE V
Va AND Ia FUNDAMENTAL AND HARMONICS

Control	I_{af}	$I_{aTHD}(\%)$	V_{af}	$V_{aTHD}(\%)$
SVPWM	135.2	2.21	489.8	3.21
MPC	134.6	1.37	503.4	0.58

VII. CONCLUSION

This paper compared SVPWM with MPC for 2L-3P VSI. MPC was found superior in terms of THD and was easier to implement.

REFERENCES

- [1] M. D. Singh, "Power Electronics," 2nd edition, Tata McGraw-Hill, 2007, ISBN:0-07-058389-7.
- [2] B. K. Boss, "Modern Power Electronics and AC Drives," Pearson Prentice Hall, 2007, ISBN:81-7758-876-1.
- [3] M. H. Rashid, "Power Electronics Circuits, Devices, and Applications," 3rd edition, Pearson Prentice Hall, 2007, ISBN:81-317-0246-4.
- [4] B. Wu, "High Power Converters and AC Drives," Wiley-IEEE Press, 2006, ISBN:0-471-731714.
- [5] Wei-Feng Zhang and Yue-Hui Yu, "Comparison of Three SVPWM Strategies," Journal of Electronic Science and Technology of China, Vol. 5, No. 3, 2007.
- [6] Advanced Energy, AE100TX, 100kW/600V three phase inverter <http://solarenergy.advanced-energy.com/> (accessed: May, 2014).